Research Article

Cancer Immunology Research

Antibody Blockade of Semaphorin 4D Promotes Immune Infiltration into Tumor and Enhances Response to Other Immunomodulatory Therapies

Elizabeth E. Evans, Alan S. Jonason Jr, Holm Bussler, Sebold Torno, Janaki Veeraraghavan, Christine Reilly, Michael A. Doherty, Jennifer Seils, Laurie A. Winter, Crystal Mallow, Renee Kirk, Alan Howell, Susan Giralico, Maria Scrivens, Katya Klimatcheva, Terrence L. Fisher, William J. Bowers, Mark Paris, Ernest S. Smith, and Maurice Zauderer

Abstract

Semaphorin 4D (SEMA4D, CD100) and its receptor plexin-B1 (PLXNB1) are broadly expressed in murine and human tumors, and their expression has been shown to correlate with invasive disease in several human tumors. SEMA4D normally functions to regulate the motility and differentiation of multiple cell types, including those of the immune, vascular, and nervous systems. In the setting of cancer, SEMA4D–PLXNB1 interactions have been reported to affect vascular stabilization and transactivation of ERBB2, but effects on immune-cell trafficking in the tumor microenvironment (TME) have not been investigated. We describe a novel immunomodulatory function of SEMA4D, whereby strong expression of SEMA4D at the invasive margins of actively growing tumors influences the infiltration and distribution of leukocytes in the TME. Antibody neutralization of SEMA4D disrupts this gradient of expression, enhances recruitment of activated monocytes and lymphocytes into the tumor, and shifts the balance of cells and cytokines toward a proinflammatory and antitumor milieu within the TME. This orchestrated change in the tumor architecture was associated with durable tumor rejection in murine Colon26 and ERBB2$^+$ mammary carcinoma models. The immunomodulatory activity of anti-SEMA4D antibody can be enhanced by combination with other immunotherapies, including immune checkpoint inhibition and chemotherapy. Strikingly, the combination of anti-SEMA4D antibody with antibody to CTLA-4 acts synergistically to promote complete tumor rejection and survival. Inhibition of SEMA4D represents a novel mechanism and therapeutic strategy to promote functional immune infiltration into the TME and inhibit tumor progression. *Cancer Immunol Res; 3(6); 689–701. ©2015 AACR.*

Introduction

Tumor growth depends on dynamic interactions within a complex ecosystem, including the proliferating neoplastic cells, immune cells, and stroma that constitute the tumor microenvironment (TME; refs. 1, 2). There is increasing evidence that effective immunotherapies can harness the immune system to promote durable tumor regression and prolong survival. To lyse neoplastic cells, leukocytes must become activated by antigen-presenting cells (APC) and gain entry into the TME, while avoiding escape mechanisms induced within the TME. Such escape mechanisms, including repulsive proteins and anergic signals, together with the architecture of the TME, modulate T-cell traffic and activation. Coordinated Th1 and cytotoxic T cell (CTL) immune infiltration into the central core and the invasive margins of human colorectal tumors (deemed "immunoscore") has been correlated with a favorable clinical outcome (3–5); however, entry of these effectors into TME is often restricted (1, 6). Increased immune infiltration into TME may enable more effective antitumor responses.

Semaphorins consist of a family of soluble and transmembrane proteins, originally defined as axonal-guidance factors (7) that also induce cytoskeletal changes in immune, endothelial, and tumor cells and guide their migration (8–10) in the TME. For example, associations of Sema3a and Neuropilin-1 have been reported to regulate movement of tumor-associated macrophages (TAM) in hypoxic regions (11). Herein, we describe a novel role for the regulation of leukocyte infiltration and tumor growth by semaphorin 4D (SEMA4D, CD100).

SEMA4D has been reported to inhibit immune-cell migration (12), and its expression may be regulated by hypoxia (13–15) and other cues within the TME. TAMs have been reported to be a necessary source of SEMA4D within the TME (16). The membrane-bound form of SEMA4D is expressed as a disulfide-linked homodimer. Upon cellular activation, the extracellular portion can be proteolytically cleaved to generate a 240-kDa soluble homodimer (17, 18). Both soluble and cell-associated forms of SEMA4D are biologically active (19). Immunohistochemical

Vaccinex, Inc., Rochester, New York.

Note: Supplementary data for this article are available at Cancer Immunology Research Online (http://cancerimmunolres.aacrjournals.org/).

Corresponding Author: Maurice Zauderer, Vaccinex, Inc., 1895 Mount Hope Avenue, Rochester, NY 14620. Phone: 585-271-2700; Fax: 585-271-2765; E-mail: mzauderer@vaccinex.com

doi: 10.1158/2326-6066.CIR-14-0171

(IHC) analysis of several tumor types revealed that both SEMA4D and its receptors are overexpressed on various human and murine tumors, including human head and neck, prostate, colon, breast, and lung cancers (20). Moreover, elevated expression correlates with invasive disease and poor prognosis in human cancer (21–25).

Three cellular receptors have been identified for SEMA4D: Plexin-B1 (PLXNB1), Plexin-B2 (PLXNB2), and CD72. PLXNB1, the highest-affinity SEMA4D receptor (K_D = 1 nmol/L), is expressed on APCs, as well as in nonlymphoid tissues, including some tumor, endothelial, and neural cells (26, 27). SEMA4D engagement with PLXNB1 has been shown to induce activation and migration of endothelial cells and regulate migration of tumor cells (26, 28). PLXNB1 binds to and can transactivate oncogenic membrane tyrosine kinases, such as cMET and ERBB2 (21, 22, 26, 28), when cross-linked by SEMA4D. PLXNB2, whose best characterized ligand is SEMA4C, also binds SEMA4D with intermediate affinity. A recent report indicates that PLXNB2 is expressed on keratinocytes and can activate SEMA4D-positive γδ T cells to contribute to epithelial wound repair (29). CD72 is a relatively low-affinity (K_D = 300 nmol/L) SEMA4D receptor (2) that is expressed primarily on B cells, APCs, and platelets (30).

Our understanding of the complex role of SEMA4D and its receptors in the process of tumor growth and metastasis is evolving. In this report, we describe the effects of antibody blockade of SEMA4D on modulation of the stroma, focusing on tumor-directed immune responses in two syngeneic tumor models. Because TAMs have been reported as a stromal source of SEMA4D (16), and the balance of M1/M2 macrophage has been identified as a prognostic factor in colon cancer (31), we selected a murine colon cancer model. In addition, given the reported role of PLXNB1 and ERBB2 interactions in oncogenic signaling (21), we also investigated the effect of anti-SEMA4D in an ERBB2-dependent mammary tumor model. We further investigate the mechanism of action by comparing and contrasting the effect of anti-SEMA4D antibody in combination with other immunomodulatory therapies.

Materials and Methods

Cell lines

Colon26 cells were purchased from the NCI (DTP, DCTD Tumor Repository, Frederick, MD) and were cultured in RPMI-1640 with 20% FBS and 0.05 mmol/L 2-mercaptoethanol. Tubo cells, a generous gift from Guido Forni (University of Torino, Italy), were cultured in DMEM with 20% FBS. Clone Tubo.A5 was isolated by FACS sorting from the Tubo cell line as a stable clone expressing high levels of rat Neu. All cells were confirmed to be *Mycoplasma* free; authentication (32) confirmed cell line identification and relation of clones to parental lines.

Mice

All mouse experiments were carried out according to the guidelines of the NIH and the University Committee on Animal Resources (UCAR) at the University of Rochester (Rochester, NY) for the care and use of laboratory animals. Female mice, 8 to 10 weeks of age, were used for all studies—BALB/cJ were purchased from Charles River or The Jackson Laboratories, and CB17 SCID were from Charles River. Some experiments were conducted at Charles River Discovery Research Services (Morrisville, NC).

Generation and purification of antibodies for *in vivo* administration

Anti-SEMA4D monoclonal antibodies (MAb) were generated following immunization of SEMA4D$^{-/-}$ mice with rSEMA4D-his. Splenocytes were fused with Sp2/0-Ag14 mouse lymphoblast cells to generate hybridomas; hybridoma clone 67-2 was selected on the basis of affinity, specificity, and functional ability to block the binding of SEMA4D to its receptors. Anti–CTLA-4 clone 4F10-UC10-11 and anti-human CD20 clone 2B8.1E7 hybridomas were obtained from the American Type Culture Collection (ATCC). 2B8.1E7, which is specific for human CD20 and does not cross-react with murine B cells, was used as an irrelevant control IgG1, isotype-matched with MAb67. Antibodies were purified from hybridoma supernatants using ProG affinity column and ion exchanges, and were confirmed to have <0.5 EU/mg endotoxin levels, ≥95% purity, and ≤5% high-molecular-weight species. Other antibody clones, including anti–PD-1/MAb RMP1-14, anti-CD8/MAb 2.43, and anti-CD4/MAb GK1.5, were purchased from BioXCell and were verified to have <2 EU/mg endotoxin levels, ≥95% purity, and ≤5% high-molecular-weight species before *in vivo* use.

In vivo tumor models and treatment

Colon26 cells (500,000) were implanted s.c. into Balb/c mice. Tubo cells (30,000) were implanted s.c. into the mammary fat pad of Balb/c mice. Similar growth kinetics were observed with 5-fold fewer Colon26 (100,000) or 2-fold fewer Tubo.A5 (15,000) cells implanted into SCID mice. Generally, 20 mice per group were implanted; mice were excluded from the analysis if sacrificed due to tumor excoriation or unexplained death before reaching endpoint tumor volume. Cyclophosphamide (Baxter) was diluted with sterile saline on each treatment day from the stock solution to provide a 50 mg/kg dose. Tumor growth was monitored using calipers two to three times per week and tumor volume (mm^3) was calculated using the formula for elliptical spheroid: $(w^2 \times l)/2$.

Immunohistochemistry

Paraformaldehyde -fixed, paraffin-embedded sections (5 μm) were stained with the following antibodies: polyclonal anti-CD8 (AbBiotec), anti-CD86 (BioSS), anti-CD20 (Epitomics), anti-FoxP3 (FJK-16s biotin-conjugated; ebioscince), anti-F4/80 (BM8; eBioscience), anti–CD206-MMR (CO68C2; BioLegend), and anti-CD11c (AP-MAB0806; Novus). Slides were imaged at ×20 magnification using a Retiga QICAM-12-bit camera (bright-field) or QICAM Aqua-16 bit (Fluorescent) coupled to an Olympus Ix50 microscope. Additional details are included in Supplementary Methods.

Functional analysis of immune cells

Cohorts of tumor-bearing mice were sacrificed at a predetermined endpoint, based on mean tumor volume (MTV) of the control group. Tumor-infiltrating leukocytes (TIL) were isolated by dissociating tissue into small pieces and digestion with 2 mg/mL collagenase D and 0.1 mg/mL DNase I for 20 minutes at 37°C. Digested tumors were then clarified by passing through a 0.07-mm cell strainer, followed by RBC lysis (Bioscience) for 5 minutes at room temperature. TILs were further enriched from tumor suspensions using Lympholyte-M (maximum of 25×10^6 cells with 5 mL Lympholyte-M), or alternatively were mixed with αCD45 microbeads (Miltenyi Biotec) and enriched into CD45$^+$

leukocytes by positive selection on an AUTOMACS column. Spleens were dissociated into small pieces and the tissue homogenate was pressed through a 0.07-mm cell strainer, followed by RBC lysis (Bioscience) for 5 minutes at room temperature.

Splenocytes and TILs were assayed by Cytometric Bead Array (CBA) cytokine analysis. Cells (200,000) were cultured in triplicate. On day 2, culture supernatants were collected. Fifty microliters of supernatant was analyzed using BD's mouse Inflammation CBA kit on a FACSCanto II flow cytometer. CBA data analysis was completed using FCAP Array software.

Colon26 splenocytes and TILs were assayed for tumor-specific $CD8^+$ responders using Mouse IFNγ ELISPOT Ready-SET-GO (Affymetrix), according to the manufacturer's instruction. Cells (5,000–10,000 TILs/well or 250,000 splenocytes/well) were plated in triplicate on MAIPS-4510 Immobilon—P membrane (Millipore) ELISPOT plates, and incubated for 18 hours at 37°C, in the presence or absence of MHC-I/H-$2L^d$–restricted immunodominant AH1 peptide of gp70 (0.01 mmol/L; ref. 33). The plates were developed using AEC (Sigma) substrate solution and analyzed by Cellular Technology Ltd.

FACS analysis

Fluorescent-conjugated rat or hamster MAbs to CD3 (clone: 17A-2), CD8a (clone: 53-6.7), CD11b (clone: M1/70), Gr-1 (clone: RB6-8C5), CD69 (clone: H1.2F3), CD25 (clone: PC61) with appropriate isotype controls were purchased from BioLegend. Samples were run on a FACSCanto II flow cytometer and analyzed using the FlowJo software.

Statistical analysis

GraphPad was used for statistical and graphical analysis. Prism reports results as statistically nonsignificant (ns) at $P > 0.05$, statistically significant at $0.01 < P \leq 0.05$ (symbolized as *), very significant (**) at $0.001 < P \leq 0.01$, and extremely significant (***) at $P \leq 0.001$. All error bars on graphs depict SEM. Additional information is included in Supplementary Data.

Results

Neutralization of SEMA4D modulates immune-cell distribution and cytokine profile within the TME

Complex interactions between the tumor and stroma, including lymphocytes and abundantly present macrophages, influence tumor growth and invasion. SEMA4D and its receptors are expressed on both tumors (Supplementary Fig. S1) and stromal cells. To evaluate the effects of SEMA4D in this complex environment, we first assessed SEMA4D expression in the TME *in situ*. Although expression of SEMA4D on Colon26 cells cultured *in vitro* was determined to be low by FACS analysis (data not shown), SEMA4D expression is strongly induced *in vivo*, forming a gradient with particularly high expression at the invasive margin of the tumor (Fig. 1 and Supplementary Fig. S2A). This area of high SEMA4D expression demarcated a striking pattern of mononuclear phagocytic cell distribution, with $F4/80^+$ cells restricted to the inner core and $CD11c^+$ cells and $CD206^+$ M2 macrophage restricted to the outer stromal edge. Anti-SEMA4D antibody blockade with murine MAb67 disrupted this gradient and was associated with increased penetration of double-positive $F4/80^+$/$CD11c^+$ inflammatory APCs and an apparent decrease in the density of protumorigenic $CD206^+$ M2 TAMs at the leading edge (Fig. 1A–D).

Concomitantly with the altered distribution of APCs, we observed increased infiltration of $CD8^+$ staining T cells into the tumor leading edge (Fig. 2A). $CD45^+$ TILs were isolated from dissociated tumors, and an increase in $CD8^+$ TILs was confirmed by FACS analysis (Fig. 2B). Functional activity of $CD8^+$ TILs was evaluated using ELISPOT to determine tumor-specific CTL activity in response to a previously identified Colon26 MHC-I–restricted immunodominant peptide, AH1 (34). Tumor peptide–specific $CD8^+$ T cells secreting IFNγ were significantly increased in tumor following *in vivo* treatment with MAb67 (Fig. 2C).

To evaluate cytokine activity associated with an increase in activated APCs following anti-SEMA4D MAb67 antibody treatment, total TILs and splenocytes were isolated from Colon26 tumor–bearing mice. TILs from mice treated with MAb67 produced higher levels of proinflammatory Th1 cytokines, IFNγ and TNFα, with a decrease in the immune-suppressive cytokine MCP-1 (Fig. 2D; ref. 35). In contrast, no statistically significant changes in cytokine levels were observed in the spleens of mice treated with MAb67 (Fig. 2E). Collectively, these data demonstrated that MAb67 enhanced APC and T-cell infiltration and promoted a Th1 cytokine milieu in the TME. The effects appear to be localized to the TME, as there was no evidence of similar activity in peripheral lymphoid tissue.

Tumor growth delay by anti-SEMA4D antibody is $CD8^+$ T cell–dependent in Colon26 tumor model

In Balb/c mice, MAb67 delayed Colon26 tumor growth and increased survival by as much as 29% ($P < 0.0001$; Fig. 3A and B). Significant tumor-growth delay (TGD), ranging from 8% to 29%, and complete tumor regression (CR) of approximately 8% were reproducible effects observed in many independent experiments performed in the Colon26 Balb/c tumor model (Table 1), both in our laboratory and as determined independently at Charles River Discovery Services. Mice that underwent complete tumor regression remained tumor free for at least 20 weeks and subsequently rejected rechallenge with homologous Colon26 tumor (Table 1). It was, therefore, striking that depletion of $CD8^+$ T cells completely abrogated antitumor effects of MAb67 treatment (Fig. 3C), indicating that CTLs are the main effectors of tumor inhibition in this model.

Despite the evidence for a changed bias in the distribution of immune subsets in TME, the effect of anti-SEMA4D/MAb67 on Colon26 tumor growth was relatively modest. We considered the possibility that the modest effect of anti-SEMA4D on tumor growth might be due to relatively low immunogenicity and a corresponding paucity of immune cells that might benefit from enhanced tumoral infiltration mediated by anti-SEMA4D antibody. In view of recent findings of durable antitumor effects of blocking immune checkpoint signals, as well as data that immunomodulatory therapies can be greatly improved when combinations are used (36, 37), we hypothesized that enhanced immune infiltration into tumor induced by anti-SEMA4D antibody may be particularly effective in combination with inhibitors of immune checkpoint blockade.

Anti-SEMA4D antibody enhances efficacy of immumomodulatory therapies anti–CTLA-4, anti–PD-1, and cyclophosphamide

The combination of anti-SEMA4D and anti–CTLA-4 antibodies was evaluated in Colon26 tumor–bearing mice. To determine additive effects in this model, a suboptimal anti–CTLA-4 regimen

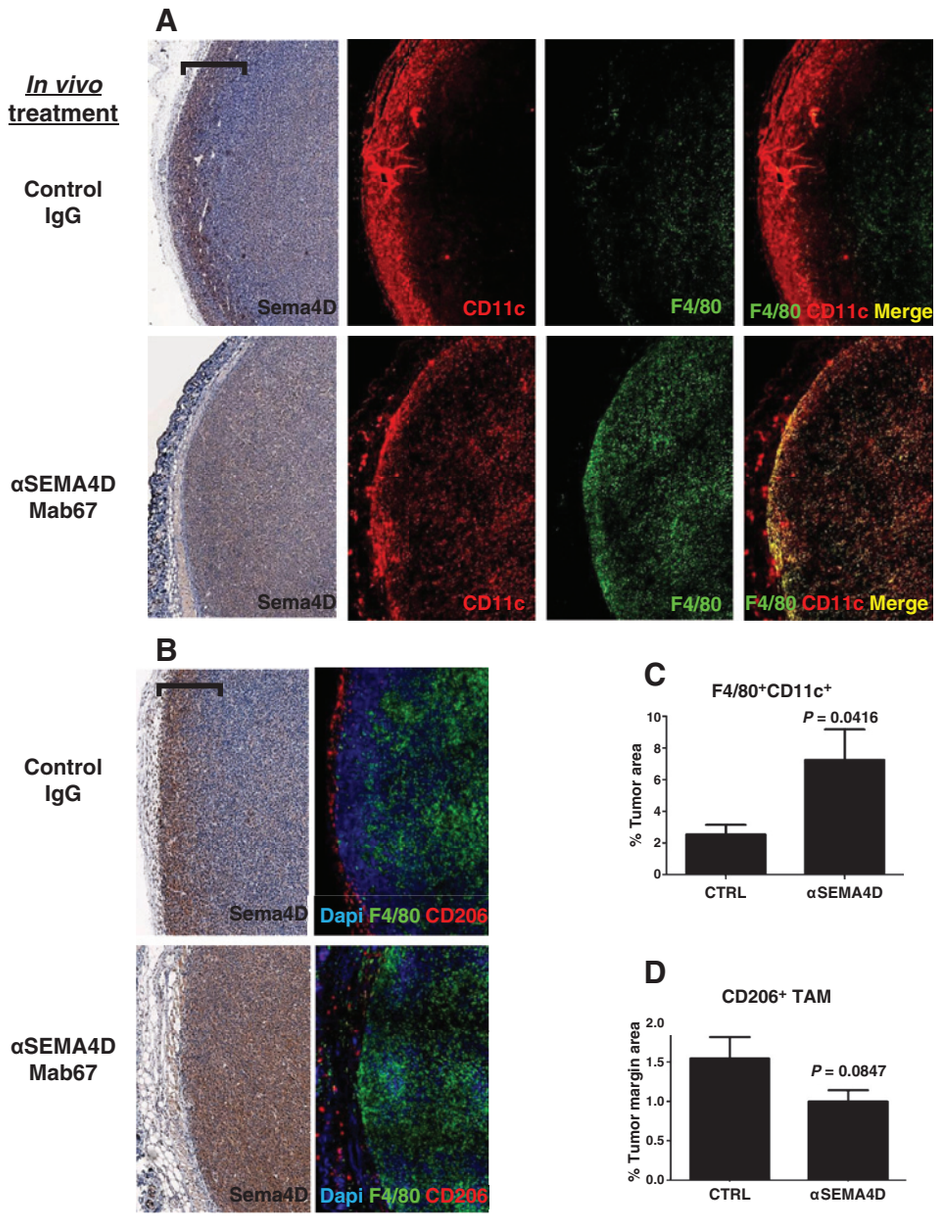

Figure 1.
Neutralization of SEMA4D gradient at the invasive tumor front allows infiltration and activation of tumor-reactive macrophage. Colon26 tumors were collected on day29 from Balb/c mice treated with control IgG1 or MAb67. Serial sections were stained for expression of A. SEMA4D (left), CD11c (red) and F4/80 (green; middle), and merge (right). B, SEMA4D (left), F4/80 (green), $CD206^+$ M2–polarized macrophages (red), with DAPI (blue) counterstain (right). A region of strongly SEMA4D-positive tumor and stroma was observed in control tumors, indicated by brackets. Both SEMA4D gradient and distribution of monocytes and T cells were altered by SEMA4D blockade. Visual assessment suggests increased infiltration of $F4/80^+CD11c^+$ DCs and a dispersal of M2-polarized $CD206^+$ TAMs away from the tumor leading edge following MAb67 treatment. Infiltration of $CD8^+$ cells (arrows) appeared to increase following MAb67 treatment, particularly at the invasive margin. For purposes of quantitation, entire tumor sections were scanned and density of stained pixel area was determined as a percentage of total tumor area (C) or the tumor margin area (D), which was defined as a 300-pixel-wide area that corresponded to the region of most intense SEMA4D staining without treatment. Group averages were calculated ($n = 10$ for each group).

was empirically determined (data not shown). As shown in Fig. 4A, under these conditions, anti–CTLA-4 as single agent resulted in 3% TGD ($P = 0.0706$). Anti-SEMA4D significantly delayed tumor growth by 9% ($P = 0.0064$) and tumors regressed in 10% of mice. Strikingly, the combination of anti–CTLA-4 with anti-SEMA4D resulted in maximum possible TGD of 114% and 85% CR ($P < 0.0001$ compared with control Ig or monotherapy treatments). It has been reported that combination with anti–PD-1 can also significantly improve the response to anti–CTLA-4 in this model (38). As a benchmark, we compared the combination of anti–CTLA-4 with anti–PD-1, resulting in 60% CR ($P < 0.0001$). The combination of anti-SEMA4D with anti–CTLA-4 was the most effective therapy in this model.

To determine whether these dramatic combination effects would translate to other immunotherapies, we tested combinations of anti-SEMA4D with either anti–PD-1 or cyclophosphamide in the Colon26 model. Figure 4B demonstrates increased efficacy when anti-SEMA4D and anti–PD-1 antibodies are combined. Using a dose of anti–PD-1 consistent with reported efficacy in this model (39), anti–PD-1 monotherapy resulted in 6% TGD ($P = 0.0483$) and 5% CR, while anti-SEMA4D/MAb67 treatment resulted in 9% TGD ($P = 0.0025$) and 5% CR. The combination of anti-SEMA4D with anti–PD-1 significantly improved the response to 67% TGD ($P < 0.0001$ compared with control and $P = 0.0025$ compared with anti–PD-1 monotherapy) and 35% CR ($P = 0.003$ compared with control and $P = 0.04$ compared with anti–PD-1 monotherapy). The additive benefit of this combination, however, contrasts with the more dramatic effect of anti-SEMA4D in combination with anti–CTLA-4. As discussed below, this is consistent with the different locus of activity of each of these agents.

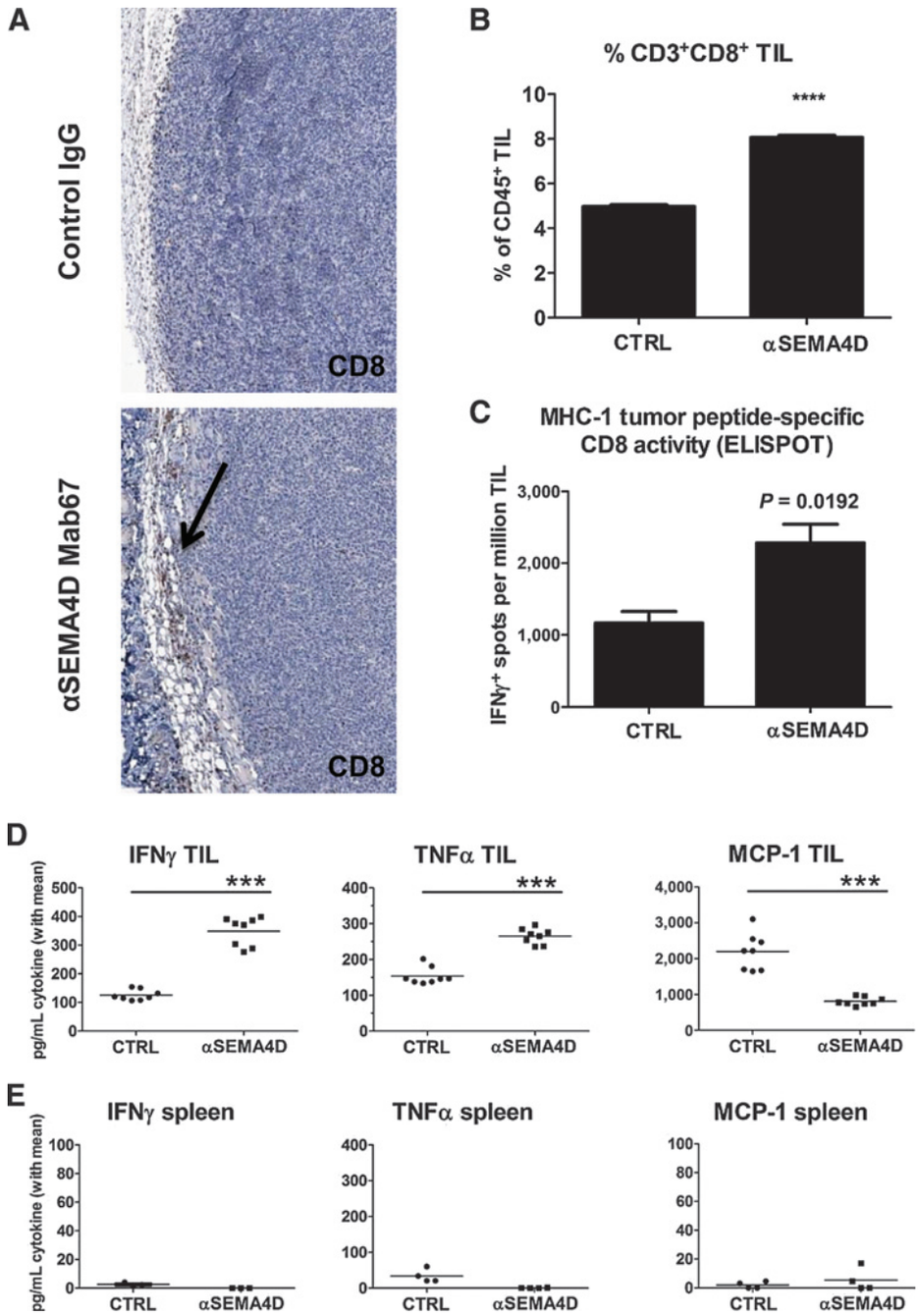

Figure 2.
Anti-SEMA4D blockade increases MHC-1–restricted, tumor peptide–specific $CD8^+$ TILs, and inflammatory Th1-type cytokines. Colon26 tumors were harvested from BALB/c mice treated *in vivo* with MAb67 or control Ig (C–E). $CD8^+$ TILs were assessed for T-cell infiltration by IHC (arrows; A) and FACS (B) on TILs from dissociated tumors; average of pooled sample replicates is shown (pooled from 6–7 mice/group). C, functional $CD8^+$ T-cell activity was assessed by incubation of pooled TILs with immunodominant MHC-1–restricted peptide AH-1 of gp70, followed by ELISPOT analysis to determine the frequency of activated IFNγ-secreting $CD8^+$ TILs. Peptide-specific response was determined by subtracting average of wells without peptide. D, pooled $CD45^+$ TILs and splenocytes were incubated for 48 hours and assayed for cytokines using CBA analysis. Statistically significant differences in IFNγ, TNFα, and MCP-1 levels were determined in the TILs of MAb67-treated mice, compared with mice treated with control Ig. E, corresponding splenocyte cytokine levels from the same mice are also shown.

Cyclophosphamide has been shown to mitigate Treg-mediated immunosuppression in rodents and in patients with cancer (34), as well as to promote immunogenic cell death and T cell–mediated immunity (40). To determine combination effects with anti-SEMA4D, a suboptimal dose of cyclophosphamide was administered 1 day before immunotherapy. Both MAb67 and cyclophosphamide significantly improved survival, with 10% and 15% CR, respectively, while the combination improved the TGD to 256% and significantly increased regression frequency to 40% CR ($P < 0.001$ for treatment effect and survival; $P = 0.0033$ for CR; Fig. 4C). Although the survival difference between cyclophosphamide monotherapy and the combination of cyclophosphamide plus MAb67 was not statistically significant ($P = 0.1$), these results suggest a trend to improved response and warrant additional studies with this and other chemotherapeutic combinations.

Anti-SEMA4D enhances antitumor immune activity of anti–CTLA-4

To further investigate the mechanism of action for the highly effective combination of anti-SEMA4D plus anti–CTLA-4, a series of experiments were conducted to assess effects on immune-cell

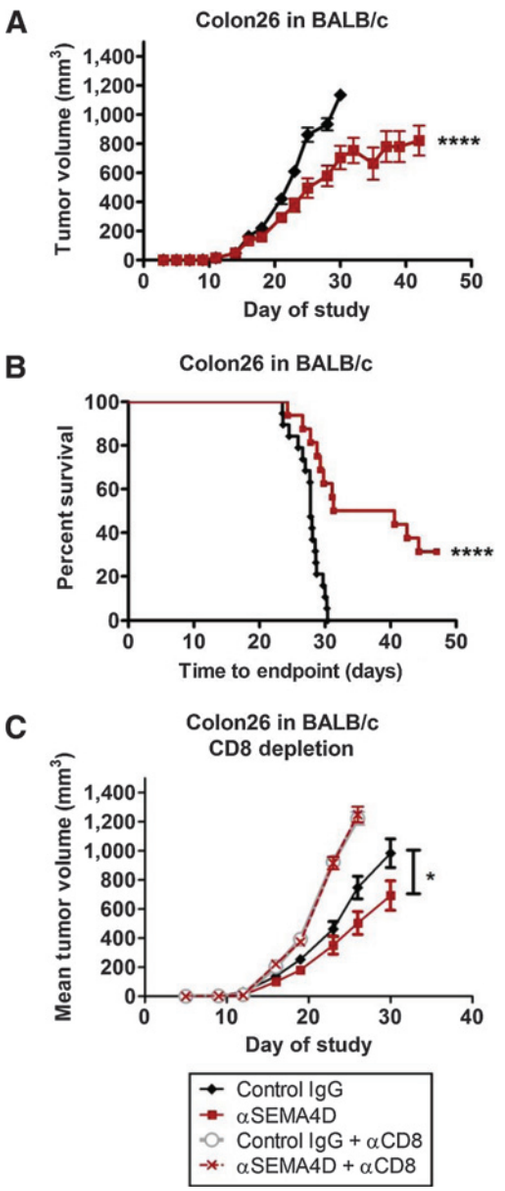

Figure 3.
Functional CD8$^+$ T cells are required for MAb67-mediated TGD. Colon26 cells were implanted s.c. into syngeneic Balb/c mice (500,000 cells). A and B, tumor-bearing mice were treated with antibodies (50 mg/kg i.p., weekly at 2 dpi): control IgG1 ($n = 18$) or MAb67 ($n = 15$). MTV (A) and Kaplan–Meier survival curve (B), using calculated time to endpoint. C, treatment with anti-SEMA4D or control IgG was initiated on day 2 (50 mg/kg i.p., weekly; $n = 20$), in combination with either anti-CD8-depleting antibody or control Rat Ig (0.15 mg i.p.), administered on days −1, 0, 1, 11, and weekly thereafter. Effective T-cell depletion was confirmed by FACS analysis on whole blood of treated mice (data not shown). MTV is shown. Thirty percent tumor growth inhibition was achieved following treatment with anti-SEMA4D; however, no treatment-related effect was observed when CD8$^+$ cells were depleted.

composition and activity in tumor. Colon26 tumor–bearing mice were sacrificed before tumor rejection, at a time when tumor volumes of treated mice were comparable (Supplementary Fig. S3). Combination therapy significantly enhanced the percentage of CD8$^+$ cells in TILs (Fig. 5A). Functional activity of these T cells was evaluated using ELISPOT (Fig. 5B). Similar to previous results, anti-SEMA4D significantly increased the frequency of tumor peptide–specific CD8$^+$ T cells secreting IFNγ within the tumor, either as a single agent or in combination with anti–CTLA-4. Although, as expected, anti–CTLA-4 antibody increased the frequency of tumor-reactive CTLs in both tumors and spleens, there was not a further increase in activated CD8$^+$ cells in the spleens of mice treated with the antibody combination, suggesting that the activity mediated by anti-SEMA4D treatment is localized to the tumor, even when combined with anti–CTLA-4 treatment. The important role of CD8$^+$ T cells in protective immunity induced by treatment with the combination of anti-SEMA4D and anti–CTLA-4 is further supported by the demonstration that in mice that have rejected tumor following such combination treatment, depletion of CD8$^+$ cells abrogates the specific immunologic memory response to a subsequent challenge with homologous tumor (Supplementary Fig. S4).

Anti–CTLA-4 therapy has been reported to increase the ratio of effector cytotoxic T cells (Teff) to suppressor regulatory T cells (Treg). Anti-SEMA4D and anti–CTLA-4 demonstrated independent and combinatorial effects on Teff to Treg ratios as determined by FACS analysis (Teff = CD8$^+$/CD69$^+$; Treg = CD4$^+$/CD25$^+$; Fig. 5C and Supplementary Fig. S5A). In support of this observation, IHC analysis using an alternate set of markers (CD8 and FoxP3) also demonstrated that the combination of anti–CTLA-4 with anti-SEMA4D significantly increased the Teff:Treg ratio compared with either monotherapy.

We also evaluated the balance of other immune cells and cytokines in this model. Anti-SEMA4D treatment increased the percentage of activated monocytes (CD86$^+$) in the tumor, while combination with anti–CTLA-4 resulted in a further and significant increase in CD86 expression relative to anti–CTLA-4 alone (Fig. 5D). Moreover, we observed a significant increase in proinflammatory cytokines, IFNγ, TNFα, and IL6, following combination therapy (Fig. 5E). Conversely, combination therapy resulted in a significant decrease in immunosuppressive cytokines MCP-1 and IL10, which were not reduced by anti–CTLA-4 therapy alone. These data suggest an orchestrated shift in the balance of pro- and anti-inflammatory signals, leading to active tumor rejection following treatment with anti-SEMA4D and anti–CTLA-4.

Collectively, these data demonstrate a novel immunomodulatory mechanism of action for SEMA4D that enhanced the activity of other immunomodulatory agents and resulted in durable tumor rejection and resistance to subsequent tumor challenge (Table 1).

SEMA4D blockade promotes tumor rejection and immunologic memory in an ERBB2$^+$ breast cancer model

Previous studies (21) have demonstrated an important role for the high-affinity PLXNB1 receptor of SEMA4D in the ERBB2 signaling pathway. It was, therefore, of interest to determine how antibody blockade of SEMA4D would affect growth in a tumor expressing ERBB2 and PLXNB1. The orthotopic Tubo.A5 murine mammary carcinoma model afforded an opportunity to investigate the interaction between immune modulation and interference with the ERBB2 signaling pathway. Strikingly, treatment of Tubo.A5 with MAb67 as a single agent resulted in maximal TGD (Fig. 6A and B and Table 1) and 86% CR, with no recurrences up to 150 days, while the median time to endpoint of the control group was 38 days. At 90 days after implant, only one mouse treated with

Table 1. Tumor regression and rechallenge summary

		Complete tumor regression				
Model	**Treatment**	**CR (%)**	**Mice (*n*) with CR/total**	**Studies (*n*)**	**Statistical significance compared with control**	**Growth after tumor rechallenge (mice)**
Colon26	Control	1	(3/278)	17	—	ND
	αSEMA4D	8	(23/298)	17	[a]	0/3
	αCTLA-4	23	(18/78)	5	[a]	1/8
	αCTLA-4 + αSEMA4D	78	(67/86)	5	[a, b]	0/32
	αPD-1	8	(3/40)	2	[a]	ND
	αPD-1 + αSEMA4D	28	(11/40)	2	[a, b]	ND
	αPD-1 + αCTLA-4	60	(12/20)	1	[a, b, c]	ND
	Cyclophosphamide	10	(3/30)	2	ns	0/3
	CY + αSEMA4D	40	(8/20)	1	[a, d]	0/8
Tubo. A5	Control	0	(0/61)	5	—	ND
	αSEMA4D	61	(56/92)	5	[a]	0/18
	αCTLA-4	23	(3/13)	1	[a]	ND
	αPD-1	0	(0/10)	1	ns	ND
	αCTLA-4 + αPD-1	14	(2/14)	1	ns	ND

NOTE: Data are compiled from several independent studies, as indicated, to demonstrate the overall frequency of tumor rejection following primary tumor graft or subsequent rechallenge. Studies include effective doses of 3–50 mg/kg MAb67; doses and schedules of other treatments are described in the text. Statistical significance of complete tumor regression (CR) was determined by the Fisher exact test. Mice with CR were challenged with viable Colon26 (500,000 cells) or Tubo. A5 (30,000 cells) in contralateral tissue at least 60 days following final treatment dose. Six naïve mice were implanted at time of rechallenge as controls for successful implant. Tumor growth was monitored for at least 30 days after challenge.

Abbreviation: ns, not statistically significant.

[a]Statistical significance between control Ig and indicated treatment group.

[b]Statistical significance between single agent aCTLA-4 and indicated treatment group.

[c]Statistical significance between single agent anti–PD-1 and indicated treatment group.

[d]Statistical significance between single agent cyclophosphamide and indicated treatment group.

MAb67 was sacrificed because of tumor burden, another tumor had shrunk from a maximum of 718 to 214 mm^3, one mouse had never developed measurable tumor, and 12 additional mice were tumor-free regressors. Similar effects were observed at doses as low as 3 mg/kg of MAb67 anti-SEMA4D antibody (Supplementary Fig. S6B), which corresponds to serum drug levels of 0.003 to 0.005 mg/mL and is also the minimal drug concentration required to fully saturate SEMA4D on circulating T cells (Supplementary Fig. S6C). This suggests that antibody saturation of SEMA4D on circulating T cells may serve as a useful PD marker in further clinical development.

To investigate immunologic memory, 12 tumor-free regressor mice were rechallenged with viable Tubo.A5 tumor in the contralateral breast tissue on day 90 (Fig. 6B). All of the MAb67-treated regressor mice rejected subsequent challenge with Tubo. A5. In other experiments, Tubo.A5 regressor mice challenged with Colon26 were unable to reject that challenge (data not shown), demonstrating that MAb67 monotherapy promoted a tumor-specific memory response (see also Table 1).

As in the Colon26 model, neutralization of a strong SEMA4D gradient at the invasive tumor front (Supplementary Fig. S2B) was associated with a shift in the balance of proinflammatory monocyte infiltration and activity, as well as increased T-cell penetration in Tubo.A5 tumors. A significant increase in $F4/80^+$/$CD11c^+$ APCs (Fig. 6C) and a concomitant significant decrease in $CD11b^+Gr1^+$ immunosuppressive myeloid-derived suppressor cells (MDSC; $P < 0.0001$) and MCP-1 cytokine secretion ($P = 0.0079$) were observed in Tubo.A5 TILs (Fig. 6D). In addition, a significant increase in the frequency of $CD3^+$ T cells ($P = 0.0012$; Fig. 6E) and a trend toward an increase in the ratio of Teffs and Tregs following treatment were also observed (Supplementary Fig. S5B).

In striking contrast to treatment of Colon26, anti-SEMA4D as a single agent resulted in maximum possible TGD and average of 61% complete tumor regression in the Tubo.A5 model. The kinetics of regression suggest that several weeks were required for an effective immune response to be induced in this model, during which time the development of an aggressive phenotype may have been held in check by blockade of the ERBB2 pathway. Accordingly, immune checkpoint blockade was found to be relatively ineffective by itself in the Tubo model (Supplementary Fig. S7A and Table 1). Anti–PD-1 was minimally effective in Tubo. A5 at doses up to 0.25 mg when administered either prophylactically at 6 dpi (data not shown) or therapeutically when tumor volume reached approximately 100 mm^3. Anti–CTLA-4 treatment was only marginally effective (23% CR, ns), and combination of the two immune checkpoint antibodies did not significantly improve responses in the Tubo model. This suggests that, in the absence of blocking the ERBB2 signaling pathway, immune resistance was not sufficient to inhibit tumor growth. The presence of an immune-independent mechanism in Tubo.A5 is further supported by the observation that MAb67 treatment induced modest, but significant, TGD in Tubo.A5 grown in SCID mice. This contrasts with results in the ERBB2-negative Colon26 model, where effects of MAb67 were completely abrogated in immune-deficient SCID mice (Supplementary Fig. S7B and S7C). Most importantly, however, the failure of tumor rejection in SCID mice highlights the requirement for lymphocytes as effectors in both models.

Discussion

These data demonstrate that SEMA4D expression at the invasive tumor edge creates a barrier to immune infiltration and biases the balance of regulatory and effector immune cells and signals. In effect, antibody-mediated SEMA4D blockade "opens the gates" to the tumor and shifts the balance toward antitumorigenic immune activity within the tumor. In two tumor models, we have

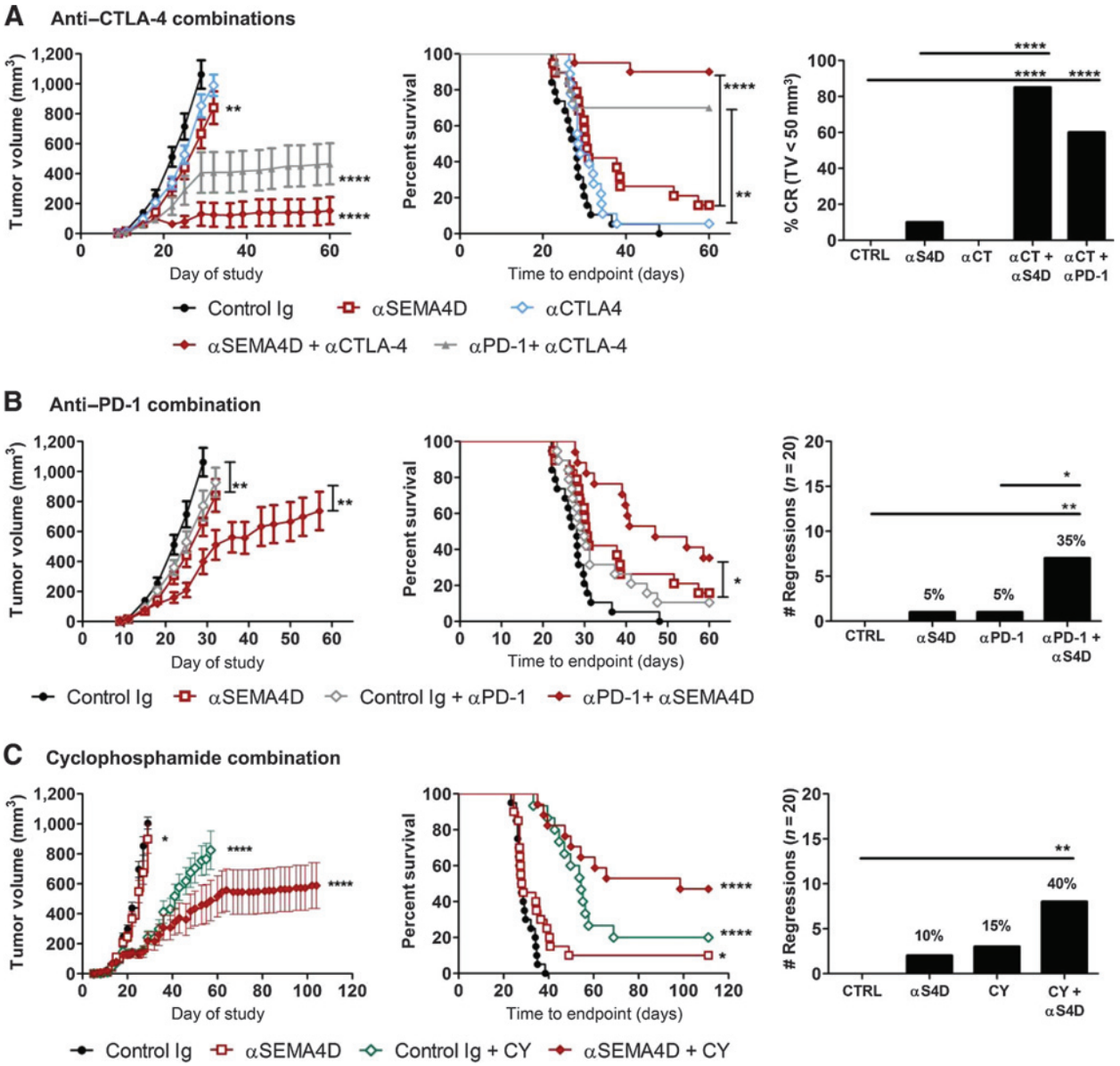

Figure 4.
Combination of anti-SEMA4D with other immunomodulatory therapies improved survival and frequency of complete tumor regression. Colon26 tumor–bearing Balb/c mice were treated, as single agents or in combinations, with anti-SEMA4D or control mouse IgG1 antibody (50 mg/kg i.p., weekly, initiated 2 dpi), anti–CTLA-4 (0.1/0.05/0.05 mg i.p., every 3 days × 3, initiated 8 dpi), anti–PD-1 (0.1 mg i.p., twice weekly at 3 dpi), and cyclophosphamide (50 mg/kg i.p., 12 and 20 dpi; $n = 18$–20/group). A, combinations with anti–CTLA-4 were significantly inhibitory compared with the control group; data shown are representative of five independent studies conducted at two independent laboratories. The combination of anti–CTLA-4 with anti-SEMA4D suggested a trend to better outcome than treatment with anti–CTLA-4 with anti–PD-1 ($P = 0.0763$). B, combination of anti–PD-1 and anti-SEMA4D was significantly inhibitory when compared with the control Ig group and when compared with anti–PD-1 monotherapy. C, combination of cyclophosphamide + anti-SEMA4D was significantly inhibitory when compared with the control Ig group. MTV, survival based on time to endpoint, and frequency of complete tumor regressions are shown. Asterisks indicate level of statistical significance: significant (*) at $0.01 < P \leq 0.05$, very significant (**) at $0.001 < P \leq 0.01$, and extremely significant (***) at $P \leq 0.001$.

described MAb67-mediated tumor rejection, corresponding with increased immune activity in the TME. Anti-SEMA4D treatment elicits a resilient antitumor response with immunologic memory, as demonstrated by durable regressions, lack of primary regrowth, or metastasis up to 17 weeks after tumor rejection, and resistance to rechallenge with the same, but not different, tumor. SEMA4D blockade represents a novel immunomodulatory mechanism to promote durable tumor rejection.

The ability of SEMA4D blockade to enhance leukocyte infiltration is consistent with reports that SEMA4D and SEMA3A can inhibit spontaneous and chemokine-induced migration of monocytes and B cells (12). The precise molecular mechanism

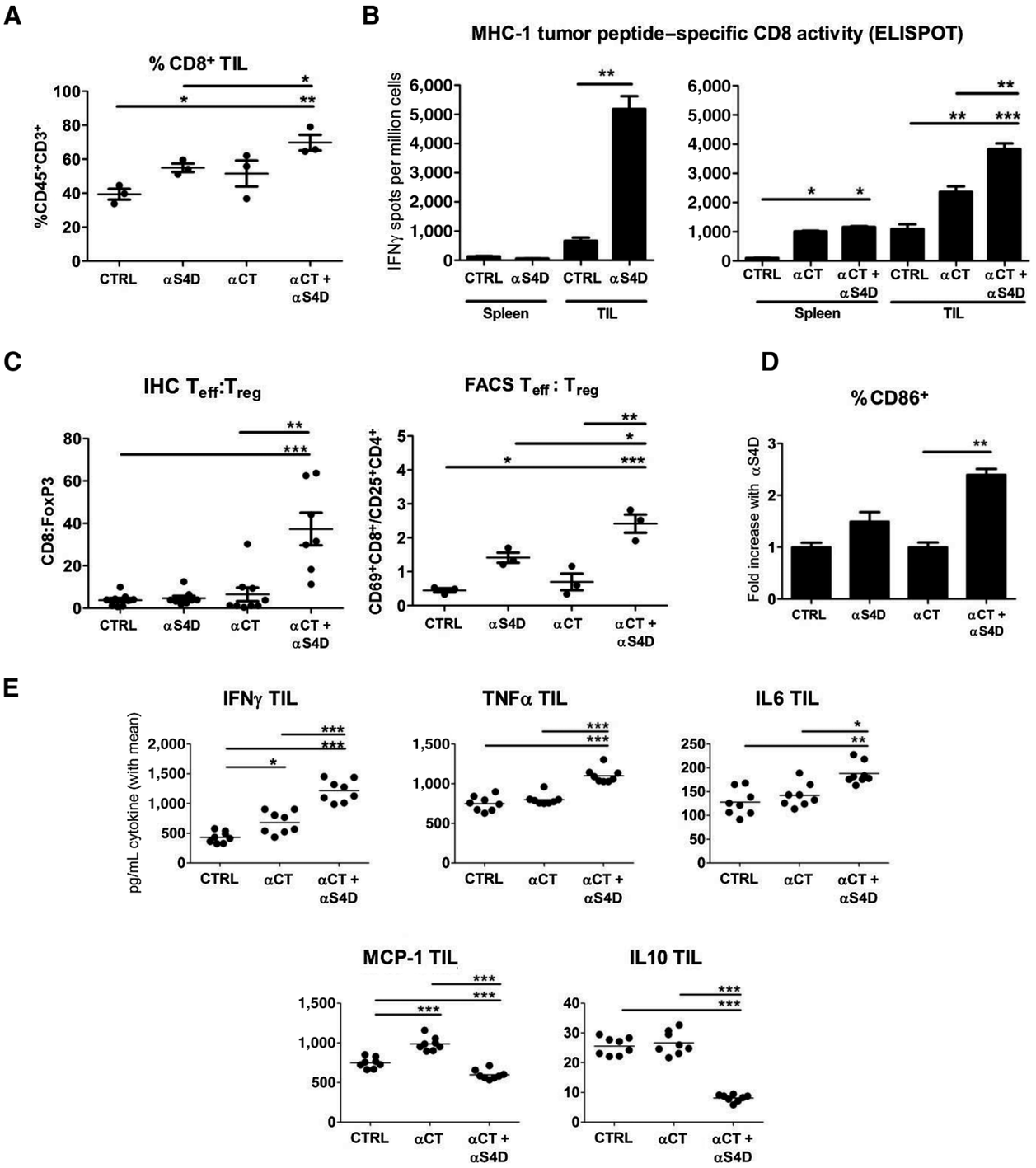

Figure 5.
Anti-SEMA4D and anti–CTLA-4 treatment is synergistic and increases the frequency of tumor-specific TILs and secretion of proinflammatory cytokines, while reducing suppressive signals. Tumors and spleens were isolated from Colon26 tumor–bearing mice following treatment. $CD45^+$ TILs were enriched from dissociated tumor using CD45 Automacs selection. Because of the small tumor volumes, it was necessary to pool samples from each treatment group for FACS and functional assays. For functional assays, TILs were pooled from 9 to 18 mice, to make up a total tumor volume of at least 1.5 g/group, and spleens were pooled from 4 to 5 mice/group; assay replicates are shown. For FACS analysis, three to four pools (3–6 tumors/pool) were assessed for each treatment group; biologic replicates are shown. Individual tumors ($n = 6$–10/group) were independently assessed by IHC and quantified using entire FFPE tumor sections, which were stained and quantitated. A, percent $CD8^+$ cells were assessed by FACS. B, IFNγ-secreting functional $CD8^+$ cells were measured by ELISPOT. C, Teff:Treg ratios were determined by FACS (left), and IHC (right); the ratio of Teff cells/Treg cells was determined for each pool or animal. D, tumor sections were also stained by IHC for monocyte-activation marker CD86. E, $CD45^+$ TILs were cultured *ex vivo* for 48 hours and assayed for cytokine secretion using CBA analysis.

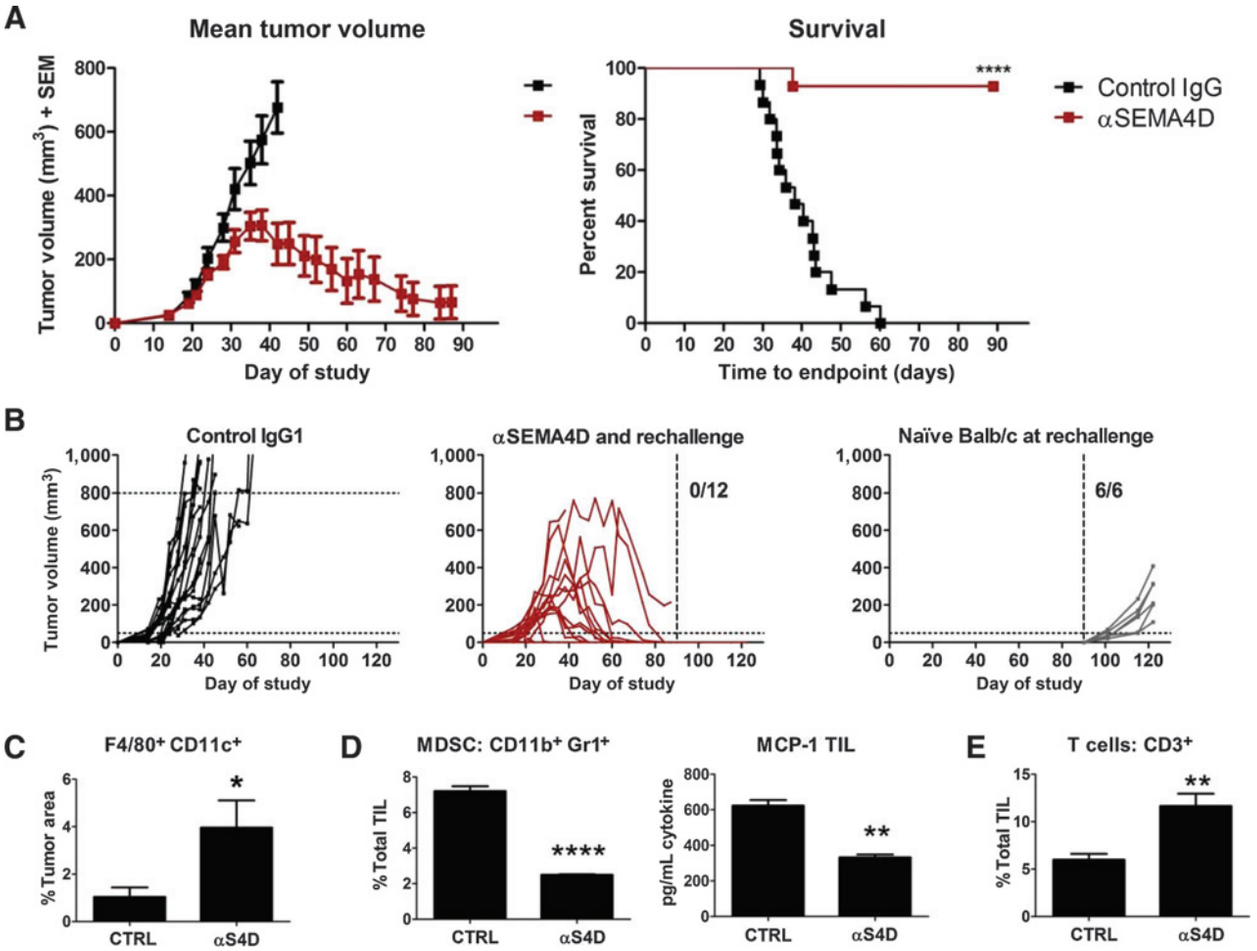

Figure 6.

Anti-SEMA4D antibody regulates immune-cell infiltration and inhibits growth of Tubo.A5 orthotopic mammary carcinoma. Tubo.A5 cells were implanted s.c. into mammary fat pad of Balb/c mice. A, weekly treatment with anti-SEMA4D/MAb67 or isotype-matched control antibodies (50 mg/kg i.p., starting 6 dpi, $n = 14$) resulted in maximal TGD of 133%**** and 86% CR****. B, tumor growth in individual mice is shown. At 90 days after implant (dotted line), 13 tumor-free mice, along with 6 naïve mice, were implanted with viable Tubo.A5 cells on the contralateral side. 0/12 mice developed tumors in MAb67-treated regressor mice, while 6 of 6 naïve mice developed tumors. Tumor-bearing animals were treated as above and tumors were harvested on day 39, before tumor rejection. At the time of harvest, the average tumor volumes were 528 and 323 mm^3 for the control and MAb67 treatment groups, respectively, resulting in 38% tumor growth inhibition ($P = 0.0015$). C, frequency of F4/80$^+$/CD11c$^+$ APCs was assessed by IHC on tumor sections. D and E, TILs were enriched using Lympholyte-M from dissociated Tubo.A5 tumors. Pooled samples were analyzed for T cells and MDSCs by FACS, and levels of MCP-1 by CBA analysis. Tubo.A5 tumors treated with MAb67 exhibit increased T-cell infiltration, with decreased levels of immunosuppressive MDSCs and MCP-1.

controlling TIL recruitment in different tumor models remains to be determined, but may be explained by several reported activities for SEMA4D, including (i) inhibition of lymphocyte migration (12), (ii) regulation of stromal components and fibrotic "wound repair" mechanisms (29), (iii) the SEMA4D–PLXNB1–RhoA signaling axis on endothelial cells regulating extravasation and/or angiogenesis (41), and (iv) the association of PLXNB1 with receptor tyrosine kinases, including ERBB2 and MET (26, 42), affecting neoplastic survival and perhaps increasing immunogenicity of the tumor.

Following SEMA4D blockade, we observed significantly reduced levels of MCP-1, which can enhance recruitment of immature monocytes into the tumor, where they may differentiate into TAMs depending on the microenvironment (43). We also observed SEMA4D-mediated effects on IL10, which can promote polarization toward a CD206$^+$ M2 phenotype and decrease expression of CD86 within the TME (35). Indeed, along with MAb67-induced reduction in IL10, we observed an increase in activated CD86$^+$ APCs with a concomitant decrease in CD11b$^+$ Gr1$^+$ MDSCs and in the density of CD206$^+$ M2 macrophages following SEMA4D blockade. Tumor-associated M2 macrophages can interact with lymphocytes to promote tumor growth; for example, TAMs can regulate the influx of CD4$^+$ Tregs and can inhibit cytotoxic CD8$^+$ T-cell responses through several mechanisms (44). MCP-1 and IL10 can also affect Teff:Treg ratios and reduce IFNγ production (45, 46). By reducing these suppressive signals, we revealed an important shift toward functional tumor-specific, IFNγ-secreting, CD8$^+$ cytotoxic T cells and an increase in the ratio of Teffs to Tregs. Increased T-cell activity also correlated with increased frequency of CD11c$^+$F4/80$^+$ APCs, which

represent potent APCs that can cross-present tumor antigens and locally activate tumor-specific T cells (47). Coordinated infiltration of $CD8^+$ and Th1 cytokine–secreting cells suggests that SEMA4D antibody blockade increases immunoscore.

The observation that anti-SEMA4D promotes immune infiltration into the TME suggested that this therapeutic might act in synergy with other immunomodulatory therapies. Indeed, anti-SEMA4D enhanced activity of several therapies reported to promote antitumor immune responses through diverse modes of action. It was striking that combination of anti-SEMA4D with anti–CTLA-4 proved more effective than combination with another immune checkpoint blockade inhibitor, anti–PD-1. Both CTLA-4 and PD-1 are upregulated on activated T cells and promote T-cell hyporesponsiveness; however, each plays a nonredundant role in modulating immune responses. CTLA-4 plays a pivotal role in attenuating the early activation of naïve and memory T cells in draining lymph nodes where the corresponding ligands, CD80 (B7-1) and CD86 (B7-2), are highly expressed. In contrast, PD-1 is primarily involved in modulating T-cell activity in tissues via its interaction with locally induced PD-L1 and PD-L2. Because anti–CTLA-4 enables greater expansion of tumor-specific T cells in draining lymph nodes in the presence of cognate ligands, B7-1 and B7-2, anti-SEMA4D antibody can act synergistically to facilitate infiltration of these expanded T cells into the tumor. In contrast, to the extent that anti–PD-1 prevents PD-L1 expressed by tumor from inactivating tumor-specific T cells that have already penetrated into the tumor environment (48), the added benefit of anti-SEMA4D in facilitating tumor infiltration may be more limited. Other immunotherapeutic interventions that activate antitumor immune responses in the periphery, such as costimulatory factors and cancer vaccines, may also benefit from disruption of immune barriers by combination with anti-SEMA4D treatment and warrant further investigation.

In the Tubo.A5 model, potent single-agent efficacy of anti-SEMA4D treatment contrasts with the need for combination therapy in the Colon26 model. Tubo.A5, unlike Colon26, expresses both PLXNB1 and ERBB2. Cross-linking of PLXNB1 by SEMA4D has been reported to transactivate ERBB2, and it has been recently reported that the ERBB2 signaling pathway must pass through PLXNB1 (42). Interference with this oncogenic pathway by anti-SEMA4D might well enhance the independent immunologic activities of this antibody by either increasing tumor immunogenicity or delaying the development of an aggressive tumor phenotype long enough for an effective immune response to be induced. The specific mechanisms of tumor growth inhibition by MAb67 in the Tubo.A5 model are currently under investigation.

The effects of anti-SEMA4D antibody treatment appear to be localized to the TME, as evidenced by changes in T-cell activity in TILs but not in the spleen, even where treatment with anti–CTLA-4 was shown to increase tumor-specific splenic T cells. This is important because, although SEMA4D is expressed on most immune cells throughout the body, our data suggest that the antibody acts locally within the tumor rather than generating systemic immunomodulatory effects, which could lead to toxicity. We have determined and report elsewhere that, while anti-SEMA4D antibody treatment can effectively saturate $SEMA4D^+$ peripheral blood mononuclear cells, it does not significantly affect peripheral peptide-specific T-cell or antibody responses, nor interfere with viral clearance (49). This is in contrast with the genetic ablation of SEMA4D early in development, which has been reported to give rise to immunologic defects (30). A simple explanation for the localized effect of anti-SEMA4D may be that the SEMA4D gradient established in tumor is not replicated in most normal tissues. This warrants further investigation. The lack of systemic immune effects by SEMA4D blockade is consistent with a favorable safety profile, which is supported by results of 6-month high-dose nonclinical toxicology in rodents and monkeys and phase I clinical testing of a humanized anti-SEMA4D antibody, VX15/MAb2503 (50).

SEMA4D blockade represents an immunotherapeutic option, with a novel and independent mechanisms of action (Supplementary Fig. S8). Other immunotherapeutic agents, including those targeting CTLA-4 and PD-1, are proving to be very effective treatment options for some cancer, resulting in complete and durable responses. As shown here, anti-SEMA4D therapy can also be effective in some tumors that do not respond to immune checkpoint blockade, such as Tubo.A5, and, importantly, can combine synergistically with immunotherapies that either reduce negative feedback, such as checkpoint blockade, or enhance immune responses, such as costimulatory activity, vaccines, or chemotherapies that induce immunogenic cell death. Results of experiments reported here demonstrate the ability of anti-SEMA4D antibody to induce a significant and durable antitumor immune response and have motivated a phase I clinical trial of a humanized anti-SEMA4D antibody, VX15/2503, in patients with solid tumors. Results of this clinical study will be reported elsewhere.

Disclosure of Potential Conflicts of Interest

M. Zauderer has ownership interest (including patents) in Vaccinex, Inc. No potential conflicts of interest were disclosed by the other authors.

Authors' Contributions

Conception and design: E.E. Evans, A.S. Jonason Jr, T.L. Fisher, E.S. Smith, M. Zauderer

Development of methodology: E.E. Evans, A.S. Jonason Jr, H. Bussler, J. Veeraraghavan, M.A. Doherty, L.A. Winter, C. Mallow, S. Giralico, K. Klimatcheva, T.L. Fisher, M. Paris

Acquisition of data (provided animals, acquired and managed patients, provided facilities, etc.): E.E. Evans, A.S. Jonason Jr, H. Bussler, S. Torno, J. Veeraraghavan, C. Reilly, M.A. Doherty, J. Seils, L.A. Winter, S. Giralico, M. Scrivens, K. Klimatcheva, W.J. Bowers, M. Paris

Analysis and interpretation of data (e.g., statistical analysis, biostatistics, computational analysis): E.E. Evans, A.S. Jonason Jr, J. Veeraraghavan, C. Reilly, M.A. Doherty, J. Seils, L.A. Winter, C. Mallow, S. Giralico, M. Scrivens, K. Klimatcheva, W.J. Bowers, M. Paris, E.S. Smith, M. Zauderer

Writing, review, and/or revision of the manuscript: E.E. Evans, A.S. Jonason Jr, C. Reilly, T.L. Fisher, W.J. Bowers, M. Paris, E.S. Smith, M. Zauderer

Administrative, technical, or material support (i.e., reporting or organizing data, constructing databases): E.E. Evans, A.S. Jonason Jr, H. Bussler, J. Veeraraghavan, C. Reilly, J. Seils, R. Kirk, A. Howell, K. Klimatcheva

Study supervision: E.E. Evans, A.S. Jonason Jr, H. Bussler, W.J. Bowers, E.S. Smith

Grant Support

This study was financially supported by Vaccinex, Inc.

The costs of publication of this article were defrayed in part by the payment of page charges. This article must therefore be hereby marked *advertisement* in accordance with 18 U.S.C. Section 1734 solely to indicate this fact.

Received September 15, 2014; revised December 23, 2014; accepted January 12, 2015; published OnlineFirst January 22, 2015.

References

1. Peranzoni E, Rivas-Caicedo A, Bougherara H, Salmon H, Donnadieu E. Positive and negative influence of the matrix architecture. Cell Mol Life Sci 2013;70:4431–48.
2. Carmeliet P. Angiogenesis in health and disease. Nat Med 2003;9:653–60.
3. Atreya I, Neurath MF. Immune cells in colorectal cancer: prognostic relevance and therapeutic strategies. Expert Rev Anticancer Ther 2008;8: 561–72.
4. Galon JA. The continuum of cancer immunosurveillance: prognostic, predictive, and mechanistic signatures. Immunity 2013;39:11–26.
5. Bindea G, Mlecnik B, Tosolini M, Kirilovsky A, Waldner M, Obenauf AC, et al. Spatiotemporal dynamics of intratumoral immune cells reveal the immune landscape in human cancer. Immunity 2013;39:782–95.
6. Hartmann N, Giese N, Giese T, Poschke I, Offringa R, Werner J, et al. Prevailing role of contact guidance in intrastromal T-cell trapping in human pancreatic cancer. Clin Cancer Res 2014;20:3422–33.
7. Giraudon P, Vincent P, Vuaillat C. T-cells in neuronal injury and repair: semaphorins and related T-cell signals. Neuromolecular Med 2005;7: 207–16.
8. Worzfeld T, Offermans S. Semaphorins and plexins as therapeutic targets. Nat Rev 2014;13:603–21.
9. Mendez-da-Cruz DA, Lepelletier Y, Brignier AC, Smaniotto S, Renand A, Milpied P, et al. Neuropilins, semaphorins, and their role in thymocyte development. Neuroimmunomodulation 2009;1153:20–8.
10. Takamatsu H, Takegahara N, Nakagawa Y, Tomura M, Taniguchi M, Friedel RH, et al. Semaphorins guide the entry of dendritic cells into the lymphatics by activating myosin II. Nat Immunol 2010;11:594–601.
11. Casazza A, Laoui D, Wenes M, Rizzolio S, Bassani N, Mambretti M, et al. Impeding macrophage entry into hypoxic tumor areas by Sema3A/Nrp1 signaling blockade inhibits angiogenesis and restores antitumor immunity. Cancer Cell 2013;24:695–709.
12. Delaire S, Billard C, Tordjman R, Chédotal A, Elhabazi A, Bensussan A, et al. Biological activity of soluble CD100. II. soluble CD100, similarly to H-SemaIII, inhibits immune cell migration. J Immunol 2001;166: 4348–54.
13. Sun Q, Zhou H, Binmadi NO, Basile JR. Hypoxia-inducible factor-1-mediated regulation of semaphorin 4D affects tumor growth and vascularity. J Biol Chem 2009;284:32066–74.
14. Bosco M, Pierobon D, Blengio F, Raggi F, Vanni C, Gattorno M, et al. Hypoxia modulates the gene expression profile of immunoregulatory receptors in human mature dendritic cells: identification of TREM-1 as a novel hypoxic marker *in vitro* and *in vivo*. Blood 2011;117: 2625–39.
15. Elvidge G, Glenny L, Appelhoff R, Ratcliffe P, Ragoussis J, Gleadle J. Concordant regulation of gene expression by hypoxia and 2-oxoglutarate-dependent dioxygenase inhibition: the role of HIF-1alpha, HIF-2alpha, and other pathways. J Biol Chem 2006;281: 15215–26.
16. Sierra JR, Corso S, Caione L, Cepero V, Conrotto P, Cignetti A. Tumor angiogenesis and progression are enhanced by Sema4D produced by tumor-associated macrophages. J Exp Med 2008;205:1673–85.
17. Kikutani H, Kumanogoh A. Semaphorins in interactions between T cells and antigen-presenting cells. Nat Rev Immunol 2003;3:159–67.
18. Basile JR, Holmbeck K, Bugge TH, Gutkind JS. MT1-MMP controls tumor-induced angiogenesis through the release of semaphorin 4D. J Biol Chem 2007;282:6899–905.
19. Hall KT, Boumsell L, Schultze JL, Boussiotis VA, Dorfman DM, Cardoso AA, et al. Human CD100, a novel leukocyte semaphorin that promotes B-cell aggregation and differentiation. Proc Natl Acad Sci U S A 1996;93: 11780–5.
20. Basile JR, Castilho RM, Williams VP, Gutkind JS. Semaphorin 4D provides a link between axon guidance processes and tumor-induced angiogenesis. Proc Natl Acad Sci U S A 2006;103:9017–22.
21. Worzfeld T, Swiercz JM, Looso M, Straub BK, Sivaraj KK, Offermanns S. ErbB-2 signals through Plexin-B1 to promote breast cancer metastasis. J Clin Invest 2012;122:1296–305.
22. Valente G, Nicotra G, Arrondini M, Castino R, Capparuccia L, Prat M, et al. Co-expression of plexin B1 and Met in human breast and ovary tumours enhances the risk of progression. Cell Oncol 2009;31:423–36.
23. Campos M, Campos SG, Ribeiro GG, Eguchi FC, Da Silva SR, De Oliveira CZ, et al. Ki-67 and CD100 immunohistochemical expression is associated with local recurrence and poor prognosis in soft tissue sarcomas, respectively. Oncol Lett 2013;5:1527–35.
24. Ch'ng ES, Kumanogoh A. Roles of Sema4D and Plexin-B1 in tumor progression. Mol Cancer 2010;9:251.
25. Kato S, Kubota K, Shimamura T, Shinohara Y, Kobayashi N, Watanabe S, et al.Semaphorin 4D, a lymphocyte semaphorin, enhancestumor cell motility through binding its receptor, plexinB1, in pancreatic cancer. Cancer Sci 2011;102:2029–37.
26. Conrotto P, Valdembri D, Corso S, Serini G, Tamagnone L, Comoglio PM, et al. Sema4D induces angiogenesis through Met recruitment by Plexin B1. Blood 2005;105:4321–9.
27. Tamagnone L, Artigiani S, Chen H, He Z, Ming GI, Song H, et al. Plexins are a large family of receptors for transmembrane, secreted, and GPI-anchored semaphorins in vertebrates. Cell 1999;99:71–80.
28. Giordano S, Corso S, Conrotto P, Artigiani S, Gilestro G, Barberis D, et al. The semaphorin 4D receptor controls invasive growth by coupling with Met. Nat Cell Biol 2002;4:720–4.
29. Witherden DA, Watanabe M, Garijo O, Rieder SE, Sarkisyan G, Cronin SJ, et al. The CD100 receptor interacts with its plexin B2 ligand to regulate epidermal gammadelta T cell function. Immunity 2012;37: 314–25.
30. Kumanogoh A, Suzuki K, Ch'ng E, Watanabe C, Marukawa S, Takegahara N, et al. Requirement for the lymphocyte semaphorin, CD100, in the induction of antigen-specific T cells and the maturation of dendritic cells. J Immunol 2002;169:1175–81.
31. Cui Y-L, Li H-K, Zhou H-Y, Zhang T, Li Q. Correlations of tumor-associated macrophage subtypes with liver metastases of colorectal cancer. Asian Pacific J Cancer Prev 2013;14:1003–7.
32. Almeida JL, Hill CR, Cole KD. Mouse cell line authentication. Cytotechnology 2014;66:133–47.
33. Huang AY. The immunodominant major histocompatibility complex class I-restricted antigen of a murine colon tumor derives from an endogenous retroviral gene product. Proc Natl Acad Sci U S A 1996;93: 9730.
34. Ghiringhelli F, Menard C, Puig PE, Ladoire S, Roux S, Martin F, et al. Metronomic cyclophosphamide regimen selectively depletes $CD4^+$ $CD25^+$ regulatory T cells and restores T and NK effector functions in end stage cancer patients. Cancer Immunol Immunother 2007;56: 641–8.
35. Lee H-W, Choi H-J, Ha S-J, Lee K-T, Kwon Y-G. Recruitment of monocytes/macrophages in different tumor microenvironments. Biochim Biophys Acta 2013;1835:170–9.
36. Page D, Postow M, Callahan M, Allison J, Wolchok J. Immune modulation in cancer with antibodies. Annu Rev Med 2014;65:185–202.
37. Harshman LC, Drake CG, Wargo JA, Sharma P, Bhardwaj N. Cancer immunotherapy highlights from the 2014 ASCO Meeting. Cancer Immunol Res 2014;2:714–9.
38. Duraiswamy J, Kaluza KM, Freeman GJ, Coukos G. Dual blockade of PD-1 and CTLA-4 combined with tumor vaccine effectively restores T-cell rejection function in tumors. Cancer Res 2013;73:3591–603.
39. Ngiow SF, von Scheidt B, Akiba H, Yagita H, Teng MW, Smyth MJ. Anti-TIM3 antibody promotes T cell IFN-g–mediated antitumor immunity and suppresses established tumors. Cancer Res 2011;71:3540–51.
40. Tongu M, Harashima N, Monma H, Inao T, Yamada T, Kawauchi H, et al. Metronomic chemotherapy with low-dose cyclophosphamide plus gemcitabine can induce anti-tumor T cell immunity *in vivo*. Cancer Immunol Immunother 2013;62:383–91.
41. Zhou H, Yang Y-H, Basile JR. The Semaphorin 4D-Plexin-B1-RhoA signaling axis recruits pericytes and regulates vascular permeability through endothelial production of PDGF-B and ANGPTL4. Angiogenesis 2013;15: 391–407.
42. Zielonka M, Krishnan R, Swiercz J, Offermans S. The IkB kinase complex is required for Plexin-B-mediated activation of RhoA. PLoS ONE 2014;9: e105661.
43. McClellan JL, Davis J, Steiner JL, Enos RT, Jung SH, Carson J A, et al. Linking tumor-associated macrophages, inflammation, and intestinal tumorigenesis: role of MCP-1. Am J Physiol Gastrointest Liver Physiol 2012;303: G1087–95.
44. Qian BZ, Pollard JW. Macrophage diversity enhances tumor progression and metastasis. Cell 2010;141:39–51.

45. Deshmane SL, Kremlev S, Amini S, Sawaya BE. Monocyte chemoattractant protein-1 (MCP-1): an overview. J Interferon Cytokine Res 2009;29:313–26.
46. Jarnicki AG, Lysaght J, Todryk S, Mills KHG. Suppression of antitumor immunity by IL-10 and TGF-producing T cells infiltrating the growing tumor: influence of tumor environment on the induction of $CD4^+$ and $CD8^+$ regulatory T cells. J Immunol 2006;177:896–904.
47. Engelhardt J, Boldajipour B, Beemiller P, Pandurangi P, Sorensen C, Werb Z, et al. Marginating dendritic cells of the tumor microenvironment cross-present tumor antigens and stably engage tumor-specific T cells. Cancer Cell 2012;21:402–17.
48. Brahmer JR, Pardoll DM. Immune checkpoint inhibitors: making immunotherapy a reality for the treatment of lung cancer. Cancer Immunol Res 2013;1:85–91.
49. Smith ES, Jonason A, Reilly C, Veeraraghavan J, Fisher T, Doherty M, et al. SEMA4D compromises blood-brain barrier, activates microglia, and inhibits remyelination in neurodegenerative disease. Neurobiol Dis 2015;73:254–68.
50. Leonard JE, Fisher TL, Winter LA, Cornelius CA, Reilly C, Smith ES, et al. Nonclinical safety evaluation of VX15/2503; a humanized IgG4 anti-SEMA4D antibody. Mol Cancer Ther 2015;14:964–72.